Large self-deflection of soliton beams in LiNb03

M. Chauvet, V. Coda, H. Maillotte, E. Fazio, G. Salamo

To be published in Optics Letters 2005

Large self-deflection of soliton beams in $LiNbO_3$

M. Chauvet, V. Coda, and H. Maillotte

Département d'Optique, Institut FEMTO-ST, UMR, CNRS, Université de Franche-Comté, 25030 Besancon, France

E. Fazio

Dipartimento di Energetica, Università La Sapienza and Istituto Nazionale per la Fisica della Materia, Via Scarpa 16, I-00161 Roma, Italy

G. Salamo

Department of Physics, University of Arkansas, Fayetteville, Arkansas 72701

Received February 15, 2005

We report the observation of large self-deflection of 2-D bright photorefractive solitons in $LiNbO_3$ crystal under a dc applied field. Beam deflection as large as 300 μm after a 7 mm propagation distance is reported, leading to formation of curved 2-D waveguides. We attribute this large deflection to the low level of impurity acceptors present in the samples, as confirmed by numerical results from a time-dependent photorefractive model.

OCIS codes: 190.0190, 190.5330, 190.5940, 160.5320, 160.2260.

In the past decade photorefractive solitons have attracted much attention. Although the first observations[1–3] and the most advanced experiments[4–6] were realized in strontium barium niobate crystal, it was recently demonstrated that $LiNbO_3$ is an excellent candidate for forming narrow bright screening spatial solitons.[7] Soliton-induced waveguides in $LiNbO_3$ have the potential to bring about new ways to design and realize photoinduced optical components. Indeed, this mature material, which is available in good optical quality with large electro-optic, nonlinear, and acousto-optic coefficients, has already found extensive application in optical components used in the optoelectronic and telecommunication industry. However, soliton-induced waveguides could make possible novel optical components and, above all, provide access to the third spatial dimension, allowing 3-D optical circuits instead of 2-D, as achieved with standard integrated technology.

In this Letter we show that self-focused beams in $LiNbO_3$ can give rise to curved photoinduced waveguides. Although beam bending has already been reported in the literature, it typically identifies a weak beam deflection of about 10–20 μm for a typical 1 cm long crystal.[8] In such experiments the deflection is essentially attributed to charge diffusion.[9] In this Letter we report the observation of a giant deflection ($\approx$300 μm) of a screening soliton in $LiNbO_3$ that depends on the amplitude of the applied field. This deflection is not due to the photorefractive charge diffusion process but instead is attributed to the low concentration of acceptor impurities present in photonic-grade $LiNbO_3$ crystals.

The optical setup is similar to that in Ref. 7. The sample used for the experiment comes from an undoped z-cut photonic-grade congruent $LiNbO_3$ wafer whose absorption at 632 nm is lower than 0.12 cm^{-1}. It is 1 mm thick along the c axis (x) and 7 mm long along the beam propagation direction (y). Electrodes are laid on the x crystal faces and the sample is placed in silicon oil to avoid arcing when an external field E_0 is applied. The light beam from a He–Ne laser at 632 nm, linearly polarized along the crystal c axis, is focused with a 70 mm focal length lens at the entrance face of the crystal to a 10 μm FWHM spot. A CCD camera in combination with an imaging lens is used to observe the beam at the exit face of the crystal.

When a positive 30 kV/cm electric field is applied along the crystal c axis, the beam diameter at the exit face gradually focuses down to 10 μm, similarly to the report in Ref. 7, and a spatial soliton is formed. However, when the same experiment is replicated using a higher applied field, intriguing beam changes are observed at the exit face. A typical observation is depicted in Fig. 1 for a 100 μW incident beam and a 50 kV/cm external applied field E_0. In the initial stage, the beam at the exit face gradually focuses [Figs. 1(a) and 1(b)] and a 10 μm diameter circular spot is reached after about 1 h. During this time a small beam shift (15 μm) opposite to the c axis is also observed. Then, in a second stage, the beam is fairly stable in position and width for a few hours [Fig. 1(c)]. Thorough examination of the beam diameter, however, reveals that the beam continues to slowly self-focus during this stage. Then the entire beam shifts and diffracts [Figs. 1(d) and 1(e)]. Subsequently, a large beam shift takes place accompanied by a refocusing effect [Figs. 1(f) and 1(g)]. Finally at steady state a tightly focused beam of about 7 μm FWHM displaced by over 200 μm in the direction opposite to the crystal c axis is formed.

For better insight, the evolution of the beam width and the position of the beam maximum have been plotted in Fig. 2 as a function of time. The only parameter that differs from the preceding experiment is the applied field, which is now set to 40 kV/cm. The general behavior is identical, but two major differences are to be noticed. First, the anomalous beam

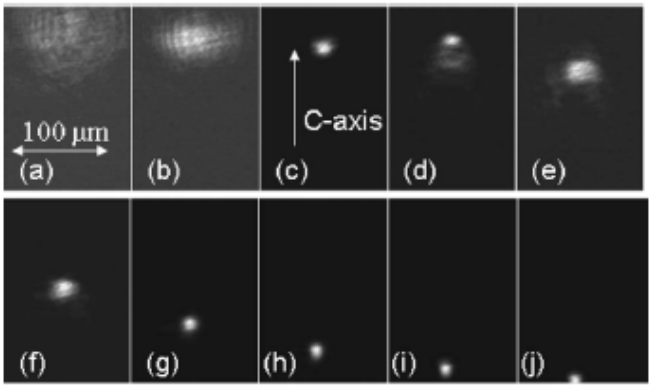

Fig. 1. Beam evolution at the exit face of a 7 mm long $LiNbO_3$ sample. Experimental parameters: E_0 =50 kV/cm, P=100 μW. Images from (a) to (j) have been taken at times, respectively, equal to 0, 0.5, 2.1, 4, 4.6, 6.3, 9.6, 13, 16.3, and 19.5 h.

shift appears later in time than for the results in Fig. 1, and, second, the total beam shift is smaller. Indeed, as a general rule, we observed that the sudden defocusing will occur sooner in time and the total shift will be larger as we increase E_0. The amplitude of the shift does not increase linearly with E_0 but tends to saturate at a high value. As a result, a 300 μm maximum shift was measured experimentally for a 60 kV/cm applied field. Note that a negative E_0 is not used since it gives rise to a defocusing effect. Besides, as is usually the case for photorefractive phenomena, the response time is inversely proportional to the incident intensity.

To understand the origin of the giant deflection we have analyzed theoretically the formation of the internal field E that is due to both the applied field E_0 and the photorefractive space-charge field. For simplicity we make use of a 1-D model with one ionization center and one carrier for which the intensity profile I is assumed to vary along the x direction. The field E, as a function of time t and spatial coordinate x, satisfies the following differential equation[10,11]:

$$\varepsilon\frac{\partial E}{\partial x\,\partial t} = -e\mu\frac{\partial (nE)}{\partial x} - \mu k_B T\frac{\partial^2 n}{\partial x^2} - \beta_{ph}(N_D - N_A)\frac{\partial I}{\partial x}, \tag{1}$$

where e and μ are, respectively, the charge and the mobility of the electron, k_B is the Boltzmann constant, T is the temperature, ε is the permittivity of the medium, and β_{ph} is the photovoltaic coefficient. N_D, N_A, and n are, respectively, the donor, acceptor, and free-electron concentrations. Equation (1) is valid for N_D or $N_A \gg n$, which is satisfied when a low light intensity is used.

If we neglect the free-electron buildup time, the density of electrons is given by[12]

$$n = A(I + I_d)\left(1 + B\frac{\partial E}{\partial x}\right)^{-1}. \tag{2}$$

Here I_d is the dark equivalent irradiance and A and B are constants, respectively, equal to $s(N_D - N_A)/\gamma N_A$ and $\varepsilon/(eN_A)$, where s is the photoexcitation cross section and γ is the carrier recombination rate. It is essential to note that in unintentionally doped crystals, such as the one used in our experiment, N_A is low, and, as a consequence, the term $B\,\partial E_{sc}/\partial x$ cannot be neglected as is usually done for doped crystals.

Integration of Eq. (1) relative to x and substitution of Eq. (2) yields, after neglecting the second-order spatial derivative of E,

$$\varepsilon\frac{\partial E}{\partial t} = -e\mu A(I + I_d)\left(1 + B\frac{\partial E}{\partial x}\right)^{-1} E - \mu k_B T A \times\left(1 + B\frac{\partial E}{\partial x}\right)^{-1}\frac{\partial I}{\partial x} - \beta_{ph}(N_D - N_A)I + D. \tag{3}$$

Since no light is present at infinite x and a uniform field E_0 is initially in place, the integration constant D is set to $e\mu A I_d E_0$. We solve Eq. (3) numerically using an iterative method considering a 10 μm FWHM Gaussian beam centered at the origin. Parameters are extracted from Ref. 13, except for N_A and N_D, which are free parameters.

Numerical results are presented in Fig. 3, where the $-E$ distribution is plotted at discrete times for two values of N_A. Since the refractive-index change is proportional to $-E$, we can picture the curves in Fig. 3 as the profile evolution of the photoinduced waveguide. The chosen reference time t_0 is equal to $2T_d I_d/I_{\max}$, where $T_d = \varepsilon\gamma N_A/[e\mu s I_d(N_D - N_A)]$ is the material dielectric response time in the dark. t_0 is the spatial soliton formation time in a quasi-steady-state regime.[11] In our experiment we can identify t_0 as the time necessary to reach the maximum self-focusing effect. The calculation reveals that the N_D concentration has little influence on the space-charge field, whereas the N_A concentration is critical. At the beginning of the process E is described by even functions for both low [Fig. 3(a)] and higher [Fig. 3(b)] N_A concentrations. Apart from a possible weak shift due to charge diffusion, the focusing effect is symmetric and the beam deflection is consequently negligible. However, as E builds up, the index profile becomes clearly asymmetric for low N_A content [Fig. 3(a)]. Al-

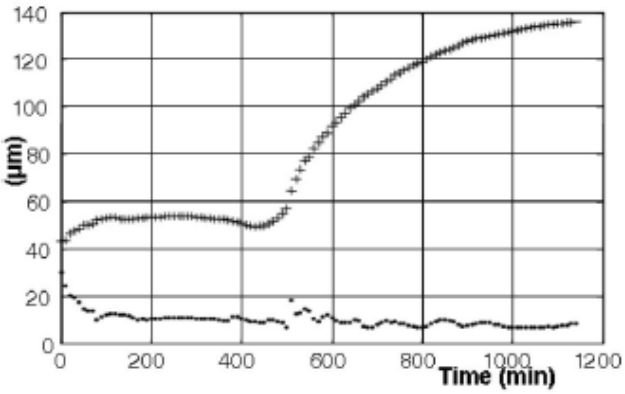

Fig. 2. Beam FWHM (dots) and position of beam maximum (crosses) versus time. Experimental parameters: E_0 =40 kV/cm, P=100 μW (the beam position curve has been arbitrarily shifted to avoid overlap).

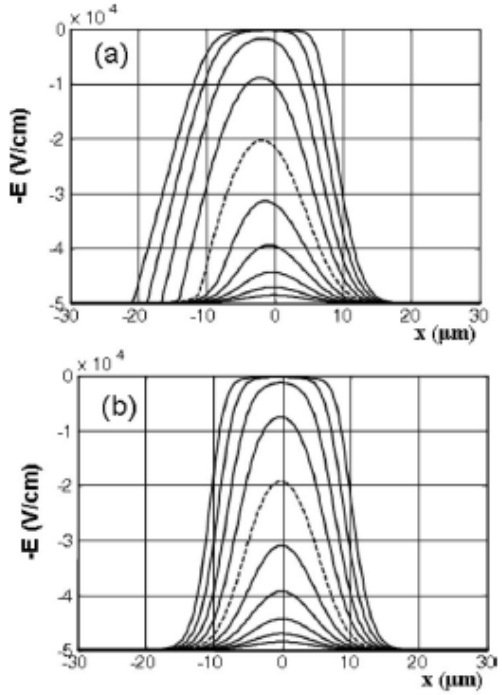

Fig. 3. Photoinduced photorefractive field distribution produced by a 10 μm FWHM Gaussian beam versus time when (a) $N_A=1\times10^{15}$ at. cm^{-3} and (b) $N_A=1\times10^{16}$ cm^{-3}. Lower curves are at $t=0.03t_0$, and time is doubled for each successive curve. Dashed curve is at $t=t_0$. Parameters: $I_{max}/I_d=10^8$, $\mu=0.74$ cm^2 V^{-1} s^{-1}, $T=290$ K, $N_D=1.1N_A$, $\gamma=1.65\times10^{-8}$ s^{-1} cm^3, $\beta_{ph}=7\times10^{-28}$ cm^3 V^{-1}, $E_0=50$ kV cm^{-1}.

though an accurate description of the influence of such an index profile on beam propagation necessitates solving the nonlinear Schrödinger equation, it is clear that beam bending opposite to the x axis will take place. Indeed, light will tend to follow the high-index region, which is now off center. In our experiments, we believe that the beam phase tilt due to this asymmetric index profile is large enough that after some propagation distance the light escapes from the initially formed waveguide, yielding the sudden partial defocusing. Moreover, since the beam is still experiencing focusing just before the abrupt change occurs, we can infer that $t<t_0$. After this stage the process is more gradual as the photoinduced waveguide adiabatically follows the light distribution change. A quasi-stable position is attained when the beam phase tilt matches the curvature of the induced waveguide. The asymmetric index profile is the direct consequence of the limited charges available to screen the applied field. It is analogous to the index grating shift observed in two-wave-mixing experiments when the applied field or the photovoltaic field is greater than the saturation field.[14]

The validity of the model is supported by experimental evidence. First, for low E_0 or at the beginning of the focusing process for higher E_0, no shift is observed because charge saturation is not reached. Second, no influence of the photovoltaic field has been noticed in our experiments, and the photovoltaic field $E_{ph}=\beta_{ph}\gamma N_A/(e\mu s)$ leads to the conclusion that N_A is indeed low. Also note that the N_A values ($\approx10^{15}$ cm^{-3}) used in the numerical calculations are realistic for unintentionally doped samples. We can even assert that the photovoltaic effect plays no role in the beam deflection. Finally, for a fixed applied field the transient defocusing appearance time is inversely proportional to the intensity. In our model, it is confirmed by the intensity dependence of t_0.

After formation of a bent soliton, the applied field and the beam can be switched off, leaving a curved waveguide in the medium. The waveguide is stored for at least several weeks in the dark and can be used to guide beams other than the original soliton beam. These low-loss bent waveguides open up new possibilities for creating complex optical circuits inside $LiNbO_3$.

In conclusion, we have shown that self-focused beams can induce the formation of curved waveguides in photonic-grade $LiNbO_3$ crystals. The curvature arises when an external field higher than a threshold value is applied on the crystal. At steady state, a beam shift as large as 300 μm is observed. We show that this unusual effect is due to a low concentration of acceptor impurity in the crystal. The space-charge field is consequently limited in amplitude and develops into an asymmetric distribution, causing the deflection. Numerical calculation of the space-charge field growth provides qualitative confirmation of this hypothesis.

This work was supported in part by the French Ministry of Education and Research through an Action Concertée Nanosciences 2004 (project NR137). M. Chauvet's e-mail address is mathieu.chauvet@univ-fcomte.fr.

References

1. M. Segev, B. Crosignani, A. Yariv, and B. Fischer, Phys. Rev. Lett. **68**, 923 (1992).
2. G. Duree, J. L. Shultz, G. Salamo, M. Segev, A. Yariv, B. Crosignani, P. Di Porto, E. Sharp, and R. R. Neurgaonkar, Phys. Rev. Lett. **71**, 533 (1993).
3. M. Shih, M. Segev, G. C. Valley, G. Salamo, B. Crosignani, and P. Di Porto, Electron. Lett. **31**, 826 (1995).
4. J. Petter and C. Denz, Opt. Commun. **188**, 55 (2001).
5. J. W. Fleischer, T. Carmon, M. Segev, N. K. Efremedis, and D. N. Christodoulides, Phys. Rev. Lett. **90**, 023902 (2003).
6. M. Klotz, H. Meng, G. J. Salamo, M. Segev, and S. R. Montgomery, Opt. Lett. **24**, 77 (1999).
7. E. Fazio, F. Renzi, R. Rinaldi, M. Bertolotti, M. Chauvet, W. Ramadan, A. Petris, and V. I. Vlad, Appl. Phys. Lett. **85**, 2193 (2004).
8. M. F. Shih, P. Leach, M. Segev, M. Garret, G. Salamo, and G. C. Valley, Opt. Lett. **21**, 324 (1996).
9. M. I. Carvalho, S. R. Singh, and D. N. Christodoulides, Opt. Commun. **120**, 311 (1995).
10. M. Chauvet, J. Opt. Soc. Am. B **20**, 2515 (2003).
11. N. Fressengeas, J. Maufoy, and G. Kugel, Phys. Rev. E **54**, 6866 (1996).
12. D. N. Christodoulides and M. I. Carvalho, J. Opt. Soc. Am. B **12**, 1628 (1995).
13. L. Ren, L. Liu, D. Liu, J. Zu, and Z. Luan, J. Opt. Soc. Am. B **20**, 2162 (2003).
14. R. A. Rupp, R. Sommerfeldt, K. H. Ringhofer, and E. Krätzig, Appl. Phys. B **51**, 364 (1990).